applied sciences

MDPI

Article

Durable Nanofiber-Based Membrane with Efficient and Consistent Performance for Oil/Saltwater Separation

Rand ElShorafa [1], Zhaoyang Liu [2,*] and Said Ahzi [3]

[1] Division of Sustainable Development, College of Science and Engineering, Hamad Bin Khalifa University, Qatar Foundation, Education City, Doha P.O. Box 34110, Qatar; relshorafa@hbku.edu.qa
[2] Qatar Environment and Energy Research Institute, Hamad Bin Khalifa University, Qatar Foundation, Doha P.O. Box 5825, Qatar
[3] ICUBE Laboratory—CNRS, University of Strasbourg, 2 Rue Boussingault, 67000 Strasbourg, France; ahzi@unistra.fr
* Correspondence: zhliu@hbku.edu.qa

Abstract: There is a large amount of oil-contaminated wastewater caused by oil/gas production and marine oil spills. It is still a major challenge for the development of oil/water separating membranes that have excellent separation efficiency, can withstand saline environments, and have long-term durability. We present a new membrane made of ultralong titanate nanofibers (TNF) (with diameter of 200 nm and length of 60 μm) and carbon nanofibers (CNF) (with a diameter of 150 nm and length of 50 μm) for efficient and consistent oil/saltwater separation. The intertwined structure of titanate and carbon nanofibers is critical to ensuring a high mechanical strength and durability for the new membrane. The carbon nanofiber works as a scaffold in this membrane to maintain mechanical integrity during multiple cycles of reuses, which is an important merit for its practical applications. The ultralong titanate nanofibers work as functional component to provide high hydrophilicity of the membrane. The new membrane has an oil/water separation efficiency of more than 99%, an oil content in treated effluent that is lower than US environmental discharge standards (42 ppm), and a high water flux of 1520 LMH/bar, due to its excellent superhydrophilicity and inter-connected pore structure. The new membrane also exhibits outstanding durability in a variety of salinity environments, as well as good resistance to oil fouling. This new type of membrane has a high potential for industrial application in treating oily wastewater due to its excellent environmental durability, oil-fouling resistance, high separation efficiency, and easy scalability.

Keywords: membrane; oil spill cleanup; filtration; durability; salty water

Citation: ElShorafa, R.; Liu, Z.; Ahzi, S. Durable Nanofiber-Based Membrane with Efficient and Consistent Performance for Oil/Saltwater Separation. *Appl. Sci.* **2023**, *13*, 6792. https://doi.org/10.3390/app13116792

Academic Editor: Francisco José Alguacil

Received: 4 April 2023
Revised: 8 May 2023
Accepted: 16 May 2023
Published: 2 June 2023

1. Introduction

Due to the enormous amounts of oily and salty wastewater produced by frequent maritime oil spill accidents as well as oil mining, production, and refinery activities, oil pollution is a serious issue on a global scale [1]. The opportunities for treating produced water are therefore increasing and driven mainly by reuse demand and regulation. The US Environmental Protection Agency (EPA) has enacted regulations that limit the amount of oil released into effluents to no more than 42 mg/L [2]. As a result, creating efficient and sustainable methods to treat wastewater that has been contaminated by oil is in high demand in order to meet stringent regulations as well as to protect the environment. Traditional oil/water separation techniques, such as hydrocyclones and air floatation, have some disadvantages, such as low separation efficiency or high operating costs [3].

Membrane techniques that operate with a "size-sieving" effect, such as nanofiltration (NF), ultrafiltration (UF), and microfiltration (MF), have been frequently utilized to purify water [4]. MF and UF membranes have limitations in terms of the size of oil droplet removal. These membranes may remove oil droplets that have micrometer size. In addition to that, MF and UF membranes can be effective in removing oil from a stable oil emulation.

Commercial UF membranes, on the other hand, have a significant fouling issue or low permeate fluxes. This is due to the fact that the pores in the UF membranes can be plugged by the oil droplets. As a result, these types of membranes have limitations in terms of service time and separation efficiency [5].

One of the major challenges in treating oily water using membrane technology is the fouling problem. Fouling is the process by which undesired particles become attached or adsorbed to the membrane which causes a reduction in the permeate flux and prevents the membrane from performing its desired application [6]. The fouling can be accumulated due to different types of foulants. Biofouling occurs when microorganisms accumulate on the membrane. In organic fouling, the foulant is an organic matter such as oil and organic chemicals. In particulate fouling, colloidal and suspended solid particles accumulate on the membrane. Scaling on membrane occurs when salts precipitate on the membrane surface.

There are two main membrane-fouling behavior types: reversible and irreversible fouling. In the reversible type, the fouling is caused by weak attachment of particles or solutes on the membrane surface or in the pores, while in irreversible fouling the physical or chemical attachments of particles or solutes are stronger than that in reversible fouling. Both types of fouling cause permeate flux decline. In reversible fouling, the flux decline can be easily recovered by water backwashing; however, in the irreversible fouling the flux decline can be recovered by washing with aggressive conditions using acid or alkali solution. Unfortunately, even after watching with aggressive conditions, the membrane cannot recover its initial permeability. For oily water treatment, scientists suggested that improving the hydrophilicity in membranes can reduce fouling [7].

Recently, superwetting membranes for efficient oil/water separation have been demonstrated by studying surface chemistry and material roughness to create superhydrophobic–superoleophilic or superhydrophilic–superoleophobic membrane surfaces [8]. It is important to examine the wetting behavior of oil as well as water on the surface of the membrane material. The wetting behavior is determined by measuring the contact angle that gives an indication about the degree of wetting when a solid and liquid interact. Materials with a contact angle lower than 90° have high wettability, while materials with a contact angle higher than 90° have low wettability. A material is said to be hydrophilic (water wet material) if the water contact angle of the material is below 90° [9]. On the other hand, a material is said to be hydrophobic (non-water wet material) if the water contact angle of the material is above 90°. Hydrophilic materials have been used in many applications including environmental applications, water treatment, and biomedical applications [9]. A superhydrophobic surface made of Teflon (PTFE)-coated mesh film has been reported for oil/water mixture separation [10]. These hydrophobic membranes, however, are easily clogged by oil. As a result of that, the permeate flux and the oil removal are inefficient. As a result, superhydrophilic and superoleophobic membranes are better suited to separate water-rich oil/water mixtures or emulsions. The majority of commercial flat sheet membranes are made of oleophilic polymers (polyvinylidene fluoride, polypropylene, and so on), which are easily fouled by oil and result in decreased separation efficiency. Simultaneously, some polyethersulfone membranes with carbon nanotube or ZnO nanofillers have been fabricated using the traditional phase inversion method for oil/water separation. However, these membranes still suffer from the problem of segregated pore structure within the membrane matrix due to the conventional membrane fabrication process [11,12]. High-energy materials with water-favoring properties were proposed for the construction of underwater superoleophobic membrane surfaces after being inspired by fish scales. Hydrogel-coated mesh, for example, was created with underwater superoleophobicity for separating oil/water mixtures and surfactant-stabilized emulsions [13,14]. However, these polymer-based approaches have shortcomings when it comes to practical applications, such as the stability of polymeric coating under harsh conditions and long-term preservation for reuse [15]. Superoleophobic membranes for oil/water separation with high separation efficiency, superior oil-fouling resistance, and high environmental durability have been used sparingly in industry up to now.

The membrane presented in this paper is made of nanofibers with interconnected porous structure with high separation efficiency for oil/saltwater emulsions and with oil residuals in the filtrates lower than environmental discharge standards (42 ppm). The high durability and performance of this nanofiber-based membrane are ensured by carbon nanofiber as mechanical scaffold and titanate nanofiber as functional materials. Meanwhile, due to its superhydrophilicity, the membrane has excellent antifouling properties. Most importantly, this new membrane has good durability in harsh environments while maintaining consistent water flux and separation efficiency. The new membrane has a small pore size that does not allow the passage of the emulsified oil through the membrane. This new membrane has a high potential for practical industrial applications due to its excellent oil/water separation efficiency, durability, fouling resistance, and low cost of fabrication. The properties of the new ultralong titanate nanofiber and carbon nanofiber membrane are described in Figure 1.

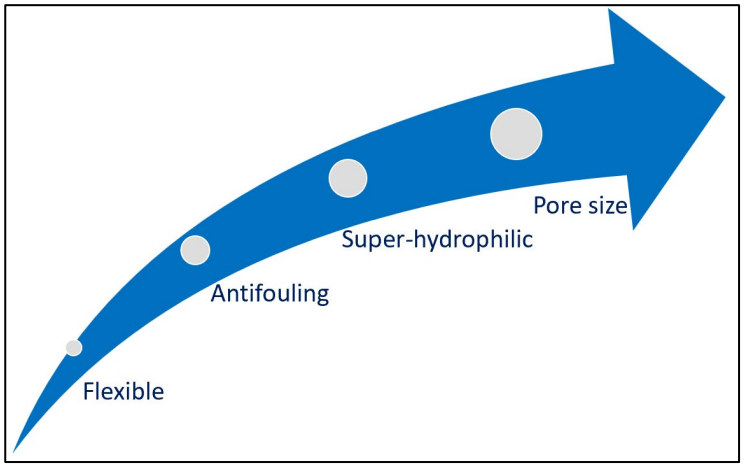

Figure 1. Properties of the new ultralong titanate nanofiber and carbon nanofiber membrane.

The technology that will be developed in this research can find numerous application opportunities such as the produced water treatment and oil spill cleanup in the sea.

- The produced water refers to the water that is returned to the surface through a well borehole. The quantity of produced water is increasing with increased volumes of global oil/gas production. This project will examine the feasibility of the synthesized membrane to treat produced water.
- Oil spills can occur in the sea and cause a negative impact on the ocean and marine life. The major human activities that cause oil spills are land drainage and waste disposal, offshore drilling, and spills from ships or tankers. These practices form a saline oily wastewater that requires a treatment process. This work will examine the feasibility of the synthesized membrane to treat saline oily water.

2. Materials and Methods

2.1. Materials

The chemicals used in this study are (Titanium dioxide (P25) (TiO_2), n-hexane C6H14, and n-Octane C_8H_{18} and were purchased from Sigma Aldrich (St. Louis, MO, USA). Carbon nanofibers were purchased from ACS Material (No. 308063-67-4) with a diameter of 150 nm and length of 50 µm. The dye of Oil Red EGN was purchased from Sigma Aldrich and was used to stain the solution to highlight the oil removing performance. In addition to that, DI water was used.

2.2. Emulsion Preparation

A stable oil-in-water emulsion was prepared using the sonication technique [16]. In this technique, an ultrasonic water bath was used to sonicate 1 mL of oil in of deionized

water of 45 mL for 5 min. A total of 100 mL of oil-in-water emulsion of 1% v/v was obtained then by diluting the emulsion with deionized water [17].

Different types of oils were used in this study to prepare the emulsion, which are sunflower oil, diesel, gasoline, n-octane, and n-hexane. To control the level of salinity content of the feed emulsion, sodium chloride was added to the emulsion to obtain salinity concentration between 2500 ppm to 45,000 ppm.

2.3. Membrane Fabrication

2.3.1. Titanium Nanofiber Synthesis

The hydrothermal method was used to fabricate titanate (Ti) nanofibers [18]. To prepare 7.5 mg/mL of TiO_2 nanoparticle (anatase P25) in 10 M NaOH solution, 0.375 g of TiO_2 nanoparticles were added and mixed for 30 min in 50 mL of a10M NaOH solution. After that, the solution was moved into an autoclave. A mechanical convection oven was set at 220 °C, and the autoclave was left in the oven for four days. Titanate nanofibers hydrogels were then formed as a result of the hydrothermal reaction between TiO_2 particles and the basic solution. After cooling the titanate nanofibers (TNF) to room temperature, the pH of the nanofibers was neutralized by washing the nanofibers with deionized water several times. Following that, the titanate nanofibers were filtered using vacuum filtration. The obtained TNF material was then allowed to dry at room temperature for 24 h prior to using the material in the membrane fabrication process. The optimization process for the deposition of different nanomaterials with 15 different compositions was shown in Figure S1.

2.3.2. Carbon Nanofiber Solution

To prepare a carbon nanofiber (CNF) solution, 10 mg of CNFs was added to 50 mL of 1% SDS solution. Probe sonication was used for 10 min to disperse the CNFs in the SDS solution. The homogenized solution was then centrifuged at 4500× g for 10 min to remove impurities such as graphitic particles and amorphous carbon.

2.3.3. Membrane Preparation

To construct TNF/CNF membrane, a pre-mixed solution containing titanium nanofibers and carbon nanofibers was applied to a cellulose substrate under low vacuum using a vacuum filtration device as presented in Figure 2.

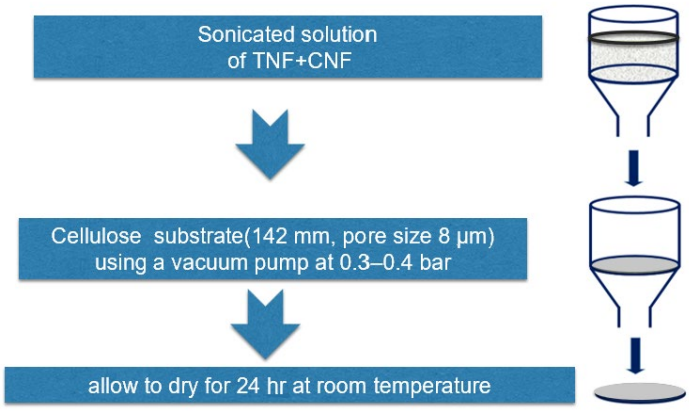

Figure 2. The fabrication process of the new TNF/CNF membrane.

To create the premixed solution, 0.08 g of TNF was mixed in 40 mL of deionized water and 1 mL of CNF. Then, the premixed solution was probe-sonicated for five minutes prior to deposition in order to homogenize the nanoparticle dispersion. The homogeneous solution was then deposited on the cellulose substrate under low vacuum using vacuum filtration. Deionized water was used to wash the deposited nanoparticles multiple times. Then, the new TNF/CNF membrane was dried at room temperature for 24 h prior to using the membrane in the performance test.

2.4. Instruments and Characterization

The water contact angle and the oil contact angle were measured to study the hydrophilicity and hydrophobicity of the membranes by using an advanced goniometer (Rame-hart A100, Arden, NC, USA). The contact angles of 5 spots on the membrane surface were measured, and the average were calculated. The surface morphology of the membrane was examined using a scanning electron microscopy (SEM, FEI Corp., Hillsboro, OR, USA) with Bruker Quantx400 EDS for microanalysis. The total organic carbon (TOC) was measured in the feed and filtrate samples using a TOC analyzer (Shimadzu, TOC-L, Tokyo, Japan). A Visual Process analyzer (JORIN-ViPA) was use to measure the size and distribution of oil droplets in the feed. The membrane material's crystal structure was investigated using an X-ray diffraction instrument (XRD, Bruker D8 Advance, Bruker-AXS, Germany).

2.5. Performance Test

The oil/water separation efficiency of the fabricated new membranes was evaluated by a filtration device (Nalgene 300–4050, Rochester, NY, USA) with its effective membrane area of 11.3 cm^2. The device was operated under vacuum filtration condition. The fabricated TNF/CNF membrane was placed in the vacuum filtration apparatus. The separation of oil and water was conducted in the dead-end filtration mode. In the filtering device, 100 mL of the prepared oil-in-water emulsions or oil-in-saline water mixtures was poured. The oil emulsion was then allowed to pass through the TNF/CNF membrane using vacuum pressure. The operating vacuum pressure throughout all the experiments was −30 KPa.

2.6. Calculation Procedure

2.6.1. Flux Calculation

Equation (1) was used to determine the fluxes through TNF/CNF membrane.

$$Flux\left(\frac{LMH}{bar}\right) = \frac{V}{StP} \quad (1)$$

where t is the testing period, P is the applied pressure, S is the membrane's surface area, and V is the volume of water permeate.

2.6.2. Oil Rejection

Equation (2) was used to determine the oil rejection when using TNF/CNF membrane.

$$R(\%) = \left(1 - \frac{Cp}{Cf}\right) \times 100 \quad (2)$$

where Cf is the feed concentration, Cp is the permeate concentration, and R is the rejection percentage. Oil concentration in the samples of feed (Cf) and of permeate (Cp) was measured using a TOC analyzer.

2.6.3. Oil Rejection

The membrane reusability was examined with ten filtration cycles. After each filtration cycle, the membrane was washed with distilled water and reused again for the next cycle. Oil concentration in the permeate was measured after each reuse cycle, and the rejection rate was calculated using Equation (2). The flux after each cycle was calculated using Equation (1).

3. Results and Discussion

We present a new nanofiber-based membrane for oil/saltwater separation in this paper. Ultralong titanate nanofiber and carbon nanofiber make up the new membrane as presented in Figure 3.

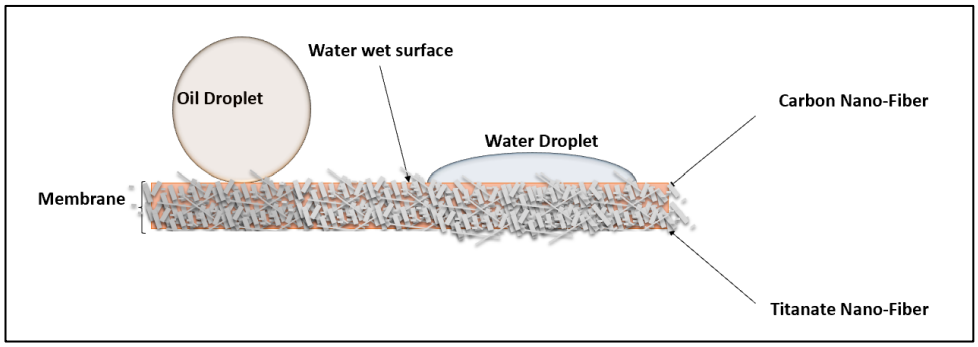

Figure 3. The new super superhydrophilic and superoleophobic ultralong titanate nanofiber and carbon nanofiber membrane.

3.1. SEM

Figure 4 represents optical SEM image of the prepared membrane. As seen in Figure 4, the long titanate nanofibers (TNF) are intertwined with the carbon nanofibers (CNF). The length and the diameter of the lab-synthesized TNFs are 60 μm and 200 nm, while the length and the diameter of the CNFs are 50 μm and 150 nm, respectively. The ultralong length of both TNF and CNF ensures the sound mechanical strength and flexibility of the membrane. The interconnected pore structure of the membrane is favorable for high permeation flux, which can be proved in the following performance tests.

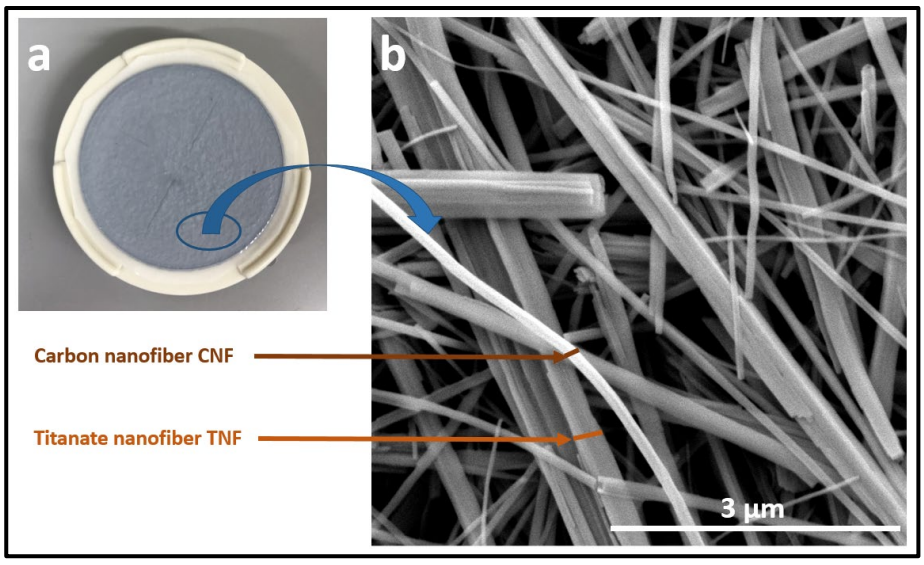

Figure 4. (**a**) Optical photo of the prepared membrane. (**b**) SEM image of the membrane materials made of titanate nanofibers and carbon nanofibers.

The porosity of the membrane was investigated by analyzing the SEM image of the membrane using Image J software [19]. As presented in Table 1, the average size of pores is 0.071 μm, and the area of the pores counts for 21.4% of the membrane area. The average pore size of the membrane is lower than the size of the emulsified oil droplet (d90 = 5.27 μm); thus, the oil cannot penetrate through the membrane, which can be proved by the following performance tests with high oil rejection rates.

Table 1. Porosity results of the membrane analyzed by Image J.

Total Area of Sample μm^2	Total Area of Pores μm^2	% of Pores Area
46.455	9.956	21.4

3.2. XRD and EDS

TiO_2 amorphous structure can be crystalized by calcination at high temperature [20]. Figure 5a represents the XRD of TNF that made up the membrane material. The peaks are marked as R for the rutile structure and A for the anatase structure as identified in the literature [21,22]. The anatase structure peaks are (101), (004), (200), and (105) which correspond to 2 theta degrees of 25.19, 38.4, 48.35, and 52.39, respectively, whereas the rutile structure peaks are (101) and (110), which correspond to 2 theta degrees of 29.4 and 35.08, respectively. The XRD of TNF matches that in the literature which proves the formation of the TNF structure from its precursor [20]. Figure 5b represents the EDS analysis of the membrane, showing the chemical elements (Ti, C, and O) of the new membranes that are made of titanate and carbon nanofibers.

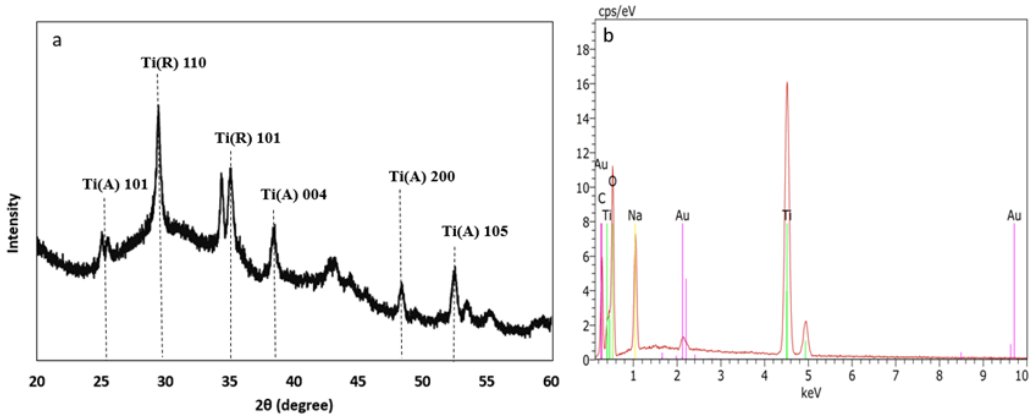

Figure 5. (**a**) XRD patterns of synthesized TNF material. (**b**) Energy Dispersive Spectroscopy (EDS) analysis of TNF/CNF membrane material, showing the chemical elements (Ti, C, and O) of the new membranes.

3.3. AFM

The purpose of performing AFM analysis of the membrane is to measure its roughness. The roughness parameters are surface kurtosis (Rku), average roughness (Ra), and root mean square roughness (Rq). Figure 6 represents the surface topography of the TNF/CNF membrane using AFM analysis. Roughness parameters of the membrane were determined from the topography image of a scanning area of 10 × 10 μm. The values of Rku, Rq, and Ra were 3.12, 5.3 nm, and 4.05 nm, respectively. The roughness parameters values were relatively low, because the relatively fine and long nanofibers were well bonded together, which results in a lower valley region in the membrane surface [23]. The stacking of fine and interpenetrated nanofibers renders the membrane with smooth surfaces. The link between surface roughness and membrane fouling during membrane filtration processes has been established [24]. The smoother the membrane surface is, the less pollutants block the valleys of the membranes, which results in less membrane fouling [25,26]. The observation of the contact angle in Figure 7 also supports the low fouling tendency, as a thin hydration layer was assumed to form on the membrane surface owing to the high hydrophilicity of the membrane, which will repel the oil pollutants from the membrane surface, as illustrated in Figure 3.

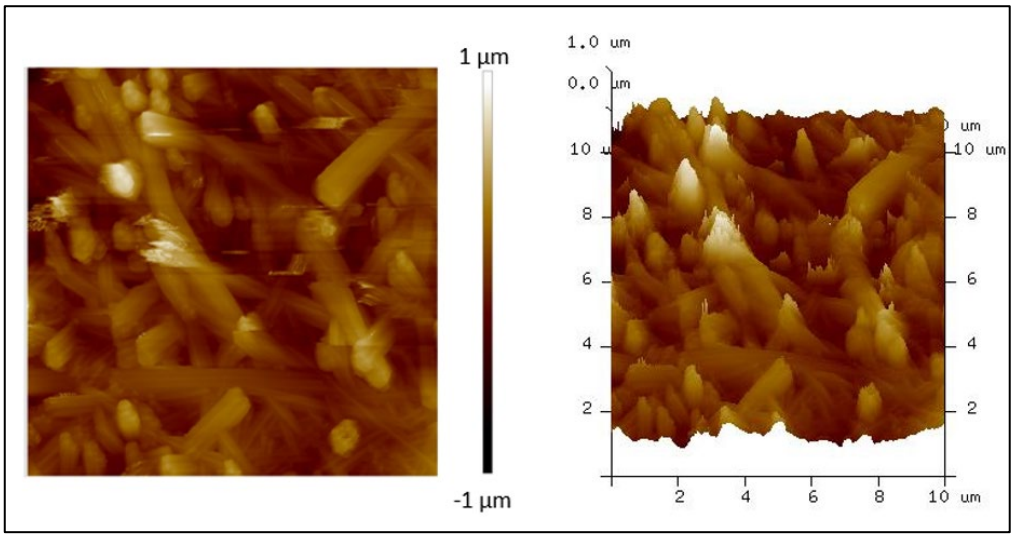

Figure 6. Surface topography of the TNF/CNF membrane using AFM analysis.

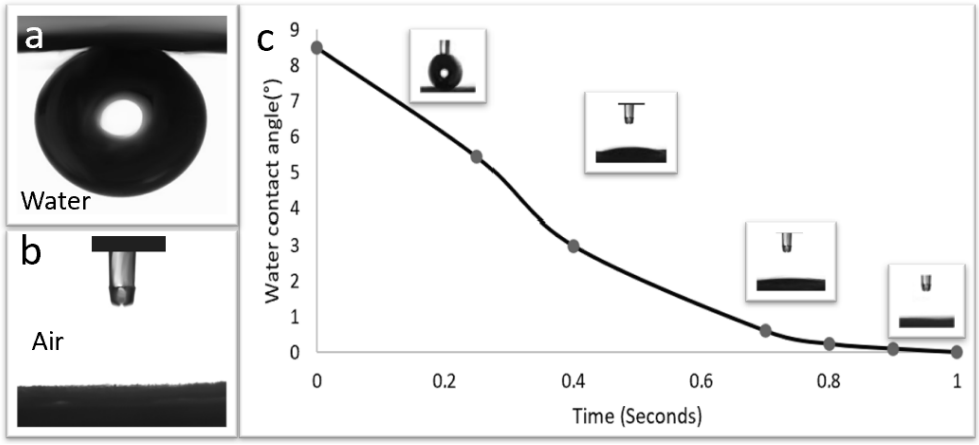

Figure 7. (**a**) Oil-in-water contact angle, (**b**) water-in-air contact angle, and (**c**) dynamic water contact angle on the new membranes.

3.4. Contact Angles for Membrane Wettability

The hydrophilicity of the membrane was identified by studying water contact angle (WCA) and oil contact angle (OCA) [27]. The dynamic water contact angle of the water droplet on the membrane surface was assisted within milliseconds. As represented in Figure 7, the water contact angle (WCA) of the TNF/CNF membrane is 0°, which implies that the membrane is superhydrophilic. Contrariwise, as represented Figure 7, the underwater oil contact angle (OCA) is 161 ± 1.5°, which indicates that the membrane is superoleophobic underwater [28]. While oil and organic substances can cause fouling on a membrane surface, the superhydrophilicity and the underwater superoleophobicity can significantly reduce the fouling of the TNF/CNF membrane. The surface free energy of the CNF/TNF membrane was investigated by using the contact angle [29]. The surface free energy of the membrane was determined to be 72.4 mN/m. The value of surface free energy is high relatively, indicating high surface polarity [29].

3.5. Performance Tests of the Membranes for the Removal of Emulsified Oil

3.5.1. Oil on Water Emulsion

One phase of oil in water emulsion is prepared prior to being used in the experiments as seen in Figure 8. The emulsified oil is characterized using ViPA. The mean size of the oil drops is 3.35 µm with d10, d50, and d90 sizes of 2.04 µm, 2.83 µm, and 5.27 µm, respectively,

as presented in Table 2. The particle mean size of the oil emulsion shows that the particle produced by the bath sonication method produces a small oil particle size that is below 20 μm.

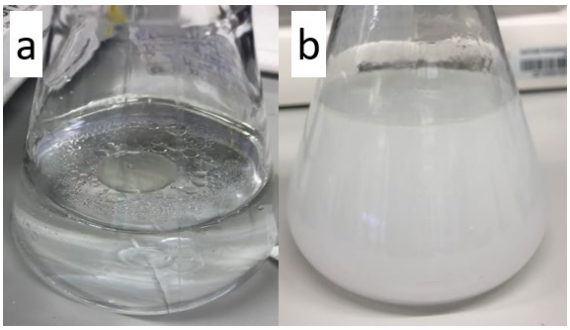

Figure 8. (**a**) Two phase oil and water mixture prior to sonication process. (**b**) One phase of oil in water emulsion after sonication process.

Table 2. Size of oil droplet in the prepared emulsion.

Mean Size (μm)	d_{10} (μm)	d_{50} (μm)	d_{90} (μm)
3.35	2.04	2.83	5.72

3.5.2. Image Characterization of the Water/Oil Solutions before and after Treatment

Figure 9 displays VIPA microscopic photograph of the oil droplets in the feed emulsion and permeate solutions. To visualize the oil emulsion in water, the oil emulsion was dyed with Oil Red EGN. Prior to filtration, the VIPA microscopic picture of the filtration exhibits the presence of oil droplets in the emulsion as observed in Figure 9a. As demonstrated in Figure 9d, oil droplets are not visible in the VIPA microscopic image after filtration, which indicates TNF/CNF membrane has removed the emulsified oil droplet from the feed.

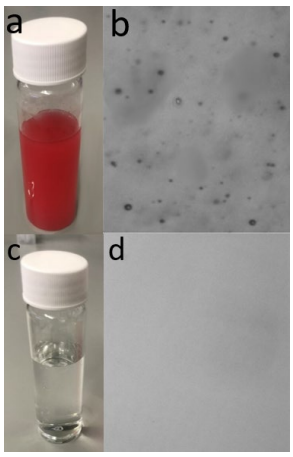

Figure 9. Oil in water emulsion before and after filtration treatment with TNF/CNF membrane. (**a**) Red dyed oil in water emulsion in the feed. (**b**) Microscopic image of oil droplet in the feed prior to filtration. (**c**) The permanent solution after using TNF/CNF membrane. (**d**) Microscopic image of the permanent solution after using TNF/CNF membrane angle.

3.5.3. Performance Tests with Different Oils

The performance of the new titanate nanofiber/carbon nanofiber (TNF/CNF) membrane was assisted using different oils in water emulsion in the feed which are vegetable oil, gasoline, engine oil, n-octane, and n-hexane. As represented in Figure 10a, the oil rejection rate exceeds 99% for the different types of oil emulsion. The oil concentration in

the permeate was less than US EPA discharge limit (42 mg/L) as presented in Figure 10b. The oil rejection rate for the different types of oil ranges between 1520 LMH/bar and 1600 LMH/bar as represented in Figure 10a.

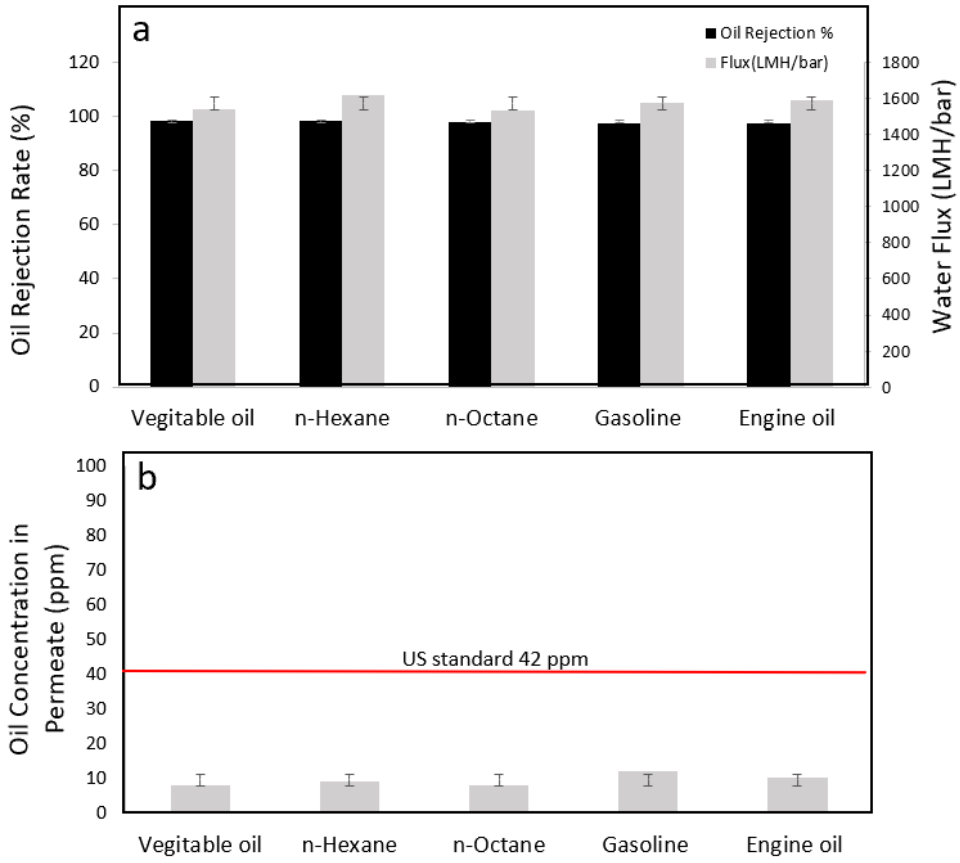

Figure 10. (**a**) Performance test (oil rejection rate and water flux (LMH/bar)) of the TNF/CNF membrane using different oil emulsions. (**b**) Oil concentration in the permeate for different types of oil.

Table 3 presents some reported data from literature of different membranes and their performance for oil/water separation. TNF/CNF membranes present a high rejection rate and water flux while having low operating pressure relatively.

Table 3. Different membranes and their performance for oil/water separation.

Membrane	Rejection Rate (%)	Flux (LMH/Bar)	Operation Pressure (KPa)	Reference
PES/CA [1]	88	6.73	400	[30]
Polysulfone	>90	1605	103.4	[31]
Ceramic ZrO_2	>90	<100	>100	[32]
TNF/CNF on cellulose paper	>99	1520	30	Current paper

[1] PES/CA is polyethersulfone/cellulosevacetate/.

3.5.4. Performance Tests with Different Salty Environments

The content of produced water and offshore oil spills has high salinity; for this reason, the performance test of TNF/CNF membrane was conducted under different saline environments. Figure 11 presents the outcome of the high salinity emulsion treatment using a TNF/CNF membrane. The percentage of oil removal was above 99% for different salty environments as represented in Figure 11a, and the oil concentration in the permeate was below 11 ppm as shown in Figure 11b, which is lower than the discharge limit of

EPA regulations. High oil rejection rate was maintained at high saline environment as presented in Figure 11a. As salts only can be dissolved in water rather than oil and the new membrane has a high separation rate between oil and water as evidenced in Figure 11, therefore there was no significant differences in terms of oil rejection rates between different salty environments. This is an indication that the membrane can function well under high saline environment. Figure S2 shows the water fluxes using TNF/CNF membrane using different loading of TNF and CNF and the percentages of oil rejection using TNF/CNF membrane using different loading of TNF and CNF.

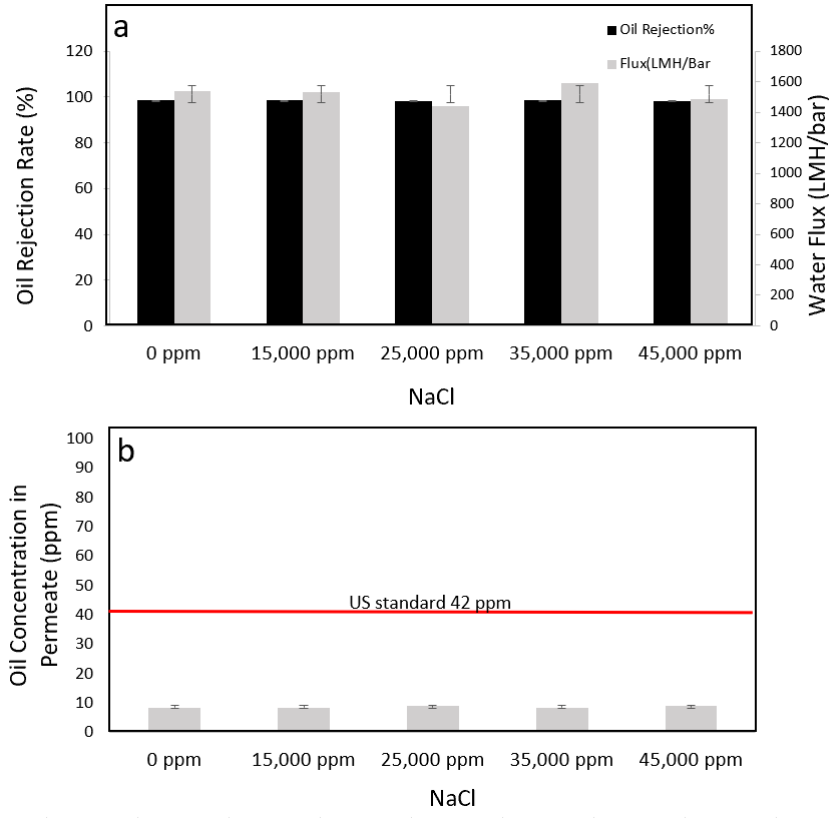

Figure 11. (**a**) Performance test (oil rejection rate and water flux (LMH/bar)) of the TNF/CNF membrane using oil emulsions with different saline environments. (**b**) Oil concentration in the permeate for oil emulsions with different saline environments.

3.5.5. Reusability Test for the Membranes

TNF/CNF membrane reusability was examined using ten filtration cycles. After each filtration cycle, the membrane was washed with distilled water and reused again for the next cycle. Oil concentration in the permeate was measured after each reuse cycle. As seen in Figure 12, throughout the 10 operating cycles, oil rejection rates were over 99% for all cycles. The permeate's oil content was consistently below the US EPA's oil disposal limit of 42 ppm. These findings show that the TNF/CNF nanocomposite membranes have excellent durability. It is worth noting that for the membrane washing, there is no need for any chemicals to be used (only distilled water used), which strongly suggests the good fouling-resistance of the membranes. The TNF/CNF membranes' superhydrophilic and oil-repellent surface can be consistently preserved. Figure S3 shows the long-term stability tests under acidic environment. Figure S4 shows the long-term stability tests under basic environment.

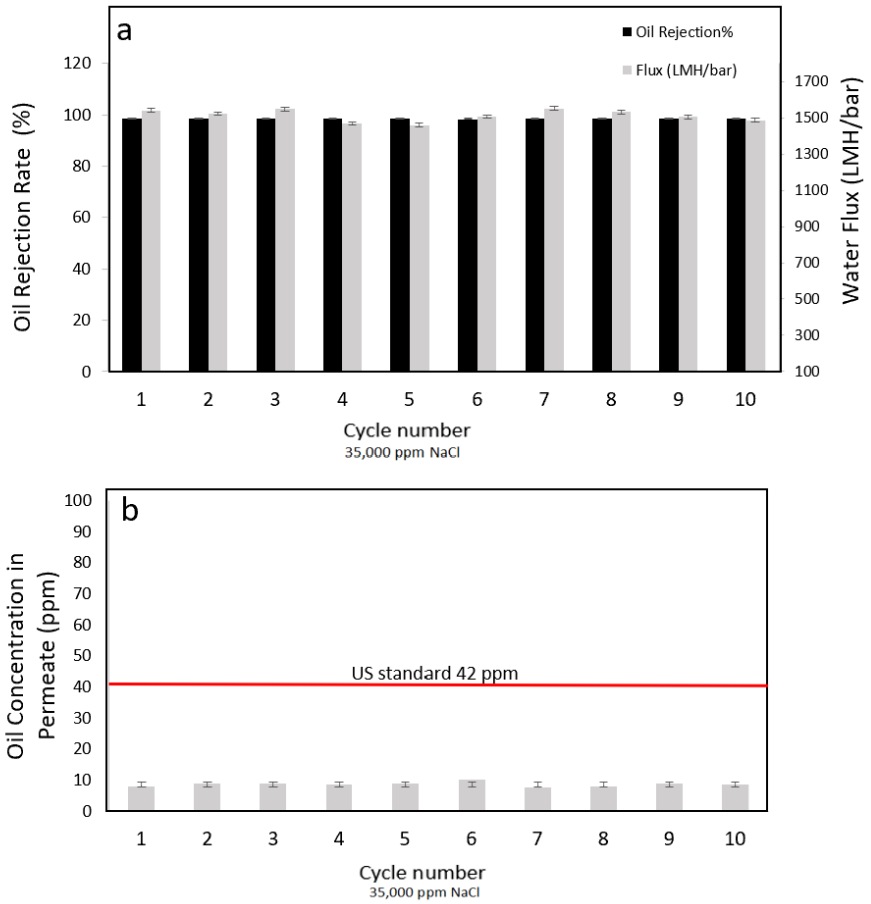

Figure 12. (**a**) The performance of the membrane after reusing the membrane 10 cycles: (**a**) oil rejection (ppm) and water flux (LMH/bar)) of the TNF/CNF membrane. (**b**) Oil concentration in the permeate after reusing the membrane 10 cycles.

4. Conclusions

For effective and reliable oil/saltwater separation, a novel type of nanostructured TNF/CNF membrane was presented in this study. The novel membranes were made of ultralong titanate and carbon nanofibers. The membranes show high hydrophilicity and high oil repellence, which render the excellent anti-oil-fouling property. The membranes feature an interconnected porous structure, which enables the high water permeation flux (1520 LMH/bar) at low operating pressure. The novel TNF/CNF membrane exhibits high oil removal above 99.1%, oil content in the permeate below the US environmental discharge limit (42 ppm). Most importantly, even after multiple cycles of reuse in environments with various salinities, the performance with oil rejection rate and water flux can be well maintained. This new membrane has great potential to treat oil/gas field production water and marine oil spills due to its durability, separation efficiency, fouling resistance, and inexpensive fabrication. The future work for this research may focus on the prototyping of the new membranes at a larger scale to further demonstrate its industrial applicability.

Supplementary Materials: The following supporting information can be downloaded at: https://www.mdpi.com/article/10.3390/app13116792/s1, Figure S1: Optimization process for the deposition of titanate nanofibers and silica solution with 15 different compositions; Figure S2: (**a**) Water Flux using TNF/CNF membrane using different loading of TNF and CNF. (**b**) Percentage of oil rejection using TNF/CNF membrane using different loading of TNF and CN; Figure S3: Long term acidic stability test (0.1 M HNO3, PH~1). (**a**) Performance test (oil rejection rate) and water flux (LMH/bar)) of the TNF/CNF mem-brane after different time interval exposure to acidic environment. (**b**) Oil concentration in the permeate different time interval exposure to acidic environment; Figure S4: Long

term basic stability test (0.1 M NaOH, PH~13). (**a**) Performance test (oil rejection rate) and water flux (LMH/bar)) of the TNF/CNF mem-brane after different time interval exposure to basic environment. (**b**) Oil concentration in the permeate different time interval exposure to basic environment.

Author Contributions: Conceptualization, R.E., Z.L. and S.A.; Methodology, R.E. and Z.L.; Validation, R.E. and Z.L.; Investigation, R.E. and Z.L.; Resources, R.E.; Writing—original draft, R.E. and Z.L.; Writing—review and editing, R.E., Z.L. and S.A. All authors have read and agreed to the published version of the manuscript.

Funding: This article has no external funding.

Informed Consent Statement: Not applicable.

Acknowledgments: The authors would like to acknowledge the contribution of the Core Laboratory of Qatar Environment and the Energy Research Institute (QEERI) for the SEM, XRD, and AFM characterizations of the materials.

Conflicts of Interest: The authors declare no conflict of interest.

References

1. Bolto, B.; Zhang, J.; Wu, X.; Xie, Z. A review on current development of membranes for oil removal from wastewaters. *Membranes* **2020**, *10*, 65. [CrossRef] [PubMed]
2. 40 CFR, Chapter 1, Environmental Protection Agency 435.1, USA, 2019. Available online: https://www.ecfr.gov/current/title-40/chapter-I/subchapter-N/part-435/subpart-A (accessed on 1 February 2023).
3. Baig, U.; Waheed, A. An efficient and simple strategy for fabricating a polypyrrole decorated ceramic-polymeric porous membrane for purification of a variety of oily wastewater streams. *Environ. Res.* **2023**, *219*, 114959. [CrossRef]
4. Gul, A.; Hruza, J.; Yalcinkaya, F. Fouling and chemical cleaning of microfiltration membranes: A mini-review. *Polymers* **2021**, *13*, 846. [CrossRef]
5. Obaid, M.; Kang, Y.; Wang, S.; Yoon, M.-H.; Kim, C.-M.; Song, J.-H.; Kim, I.S. Fabrication of highly permeable thin-film nanocomposite forward osmosis membranes via the design of novel freestanding robust nanofiber substrates. *J. Mater. Chem. A* **2018**, *6*, 11700–11713. [CrossRef]
6. Tummons, E.; Han, Q.; Tanudjaja, H.J.; Hejase, C.A.; Chew, J.W.; Tarabara, V.V. Membrane fouling by emulsified oil: A review. *Sep. Purif. Technol.* **2020**, *248*, 116919. [CrossRef]
7. Dmitrieva, E.S.; Anokhina, T.S.; Novitsky, E.G.; Volkov, V.V.; Borisov, I.L.; Volkov, A.V. Polymeric Membranes for Oil-Water Separation: A Review. *Polymers* **2022**, *14*, 980. [CrossRef] [PubMed]
8. Yong, J.; Yang, Q.; Hou, X.; Chen, F. Emerging Separation Applications of Surface Superwettability. *Nanomaterials* **2022**, *12*, 688. [CrossRef]
9. Matindi, C.N.; Kadanyo, S.; Liu, G.; Hu, M.; Hu, Y.; Cui, Z.; Ma, X.; Yan, F.; He, B.; Li, J. Hydrophilic polyethyleneimine-TiO_2 hybrid layer on polyethersulfone/sulfonated polysulfone blend membrane with antifouling characteristics for the effective separation of oil-in-water emulsions. *J. Water Process Eng.* **2022**, *49*, 102982. [CrossRef]
10. Fen, L.; Zhang, Z.; Mai, Z.; Ma, Y.; Liu, B.; Jiang, L.; Zhu, D. A super-hydrophobic and super-oleophilic coating mesh film for the separation of oil and water. *Angew. Chem. Int. Ed.* **2004**, *43*, 2012–2014. [CrossRef]
11. Kusworo, T.D.; Qudratun; Utomo, D.P. Performance evaluation of double stage process using nano hybrid PES/SiO_2-PES membrane and PES/ZnO-PES membranes for oily waste water treatment to clean water. *J. Environ. Chem. Eng.* **2017**, *5*, 6077–6086. [CrossRef]
12. Omalanga, L.; Iyuke, S.; Nkazi, B.; Biyela, P. Impact of Carbon Nanotubes on the Polymeric Membrane for Oil—Water Separation. *Int. J. Nanosci. Nanotechnol.* **2019**, *15*, 99–115. Available online: https://www.ijnnonline.net/article_35420.html (accessed on 1 April 2023).
13. Xue, Z.; Wang, S.; Lin, L.; Chen, L.; Liu, M.; Feng, L.; Jiang, L. A novel superhydrophilic and underwater superoleophobic hydrogel-coated mesh for oil/water separation. *Adv. Mater.* **2011**, *23*, 4270–4273. [CrossRef] [PubMed]
14. Zhang, Q.; Liu, N.; Wei, Y.; Feng, L. Facile fabrication of hydrogel coated membrane for controllable and selective oil-in-water emulsion separation. *Soft Matter* **2018**, *14*, 2649–2654. [CrossRef] [PubMed]
15. Sun, H.; Zhang, Y.; Sadam, H.; Ma, J.; Bai, Y.; Shen, X.; Kim, J.-K.; Shao, L. Novel mussel-inspired zwitterionic hydrophilic polymer to boost membrane water-treatment performance. *J. Membr. Sci.* **2019**, *582*, 1–8. [CrossRef]
16. Sakai, T. Surfactant-free emulsions. *Curr. Opin. Colloid Interface Sci.* **2008**, *13*, 228–235. [CrossRef]
17. Fard, A.K.; Bukenhoudt, A.; Jacobs, M.; McKay, G.; Atieh, M.A. Novel hybrid ceramic/carbon membrane for oil removal. *J. Membr. Sci.* **2018**, *559*, 42–53. [CrossRef]
18. Jung, S.M.; Jung, H.Y.; Fang, W.; Dresselhaus, M.S.; Kong, J. A Facile Methodology for the Production of In Situ Inorganic Nanowire Hydrogels/Aerogels. *Nano Lett.* **2014**, *14*, 1810–1817. [CrossRef]
19. Sun, W.; Chen, T.; Chen, C.; Li, J. A study on membrane morphology by digital image processing. *J. Membr. Sci.* **2007**, *305*, 93–102. [CrossRef]

20. Kim, J.-H.; Lee, J.-H.; Kim, J.-Y.; Kim, S.S. Synthesis of aligned TiO_2 nanofibers using electrospinning. *Appl. Sci.* **2018**, *8*, 309. [CrossRef]
21. Sikhwivhilu, L.M.; Mpelane, S.; Moloto, N.; Ray, S.S. Hydrothermal Synthesis of TiO_2 Nanotubes: Microwave Heating Versus Conventional Heating. *Nanostruct. Mater. Nanotechnol. IV Ceram. Eng. Sci. Proc.* **2010**, *31*, 45–49.
22. Yoon, S.H.; ElShorafa, R.; Katbeh, M.; Han, D.S.; Jeong, H.W.; Park, H.; Abdel-Wahab, A. Effect of shape-driven intrinsic surface defects on photocatalytic activities of titanium dioxide in environmental application. *Appl. Surf. Sci.* **2017**, *423*, 71–77. [CrossRef]
23. Rajasekhar, T.; Trinadh, M.; Babu, P.V.; Sainath, A.V.S.; Reddy, A.V.R. Oil-water emulsion separation using ultrafiltration membranes based on novel blends of poly(vinylidene fluoride) and amphiphilic tri-block copolymer containing carboxylic acid functional group. *J. Membr. Sci.* **2015**, *481*, 82–93. [CrossRef]
24. Barambu, N.U.; Bilad, M.R.; Wibisono, Y.; Jaafar, J.; Mahlia, T.M.I.; Khan, A.L. Membrane surface patterning as a fouling mitigation strategy in liquid filtration: A review. *Polymers* **2019**, *11*, 1687. [CrossRef]
25. Vrijenhoek, E.M.; Hong, S.; Elimelech, M. Influence of membrane surface properties on initial rate of colloidal fouling of reverse osmosis and nanofiltration membranes. *J. Memb. Sci.* **2001**, *188*, 115–128. [CrossRef]
26. Elimelech, M.; Zhu, X.; Childress, A.E.; Hong, S. Role of membrane surface morphology in colloidal fouling of cellulose acetate and composite aromatic polyamide reverse osmosis membranes. *J. Memb. Sci.* **1997**, *127*, 101–109. [CrossRef]
27. Liu, Y.; Coppens, M.O. Cell Membrane-Inspired Graphene Nanomesh Membrane for Fast Separation of Oil-in-Water Emulsions. *Adv. Funct. Mater.* **2022**, *32*, 2200199. [CrossRef]
28. Elshorafa, R.; Saththasivam, J.; Liu, Z.; Ahzi, S. Efficient oil/saltwater separation using a highly permeable and fouling-resistant all-inorganic nanocomposite membrane. *Environ. Sci. Pollut. Res.* **2020**, *27*, 15488–15497. [CrossRef]
29. Hashim, I.A.; Aisueni, F.; Ogunlude, P.; Ramalan, M.; Ogoun, E.; Gobina, E. Using contact angle measurements for determination of the surface free energy of ceramic membranes. *TechConnect Briefs* **2022**, *44*, 5–8.
30. Mansourizadeh, A.; Azad, A.J. Preparation of blend polyethersulfone/cellulose acetate/polyethylene glycolasymmetric membranes for oil–water separation. *J. Polym. Res.* **2014**, *21*, 375. [CrossRef]
31. Chakrabarty, B.; Ghoshal, A.K.; Purkait, M.K. Purkait, Ultrafiltration of stable oil-in-water emulsion by polysulfone membrane. *J. Membr. Sci.* **2008**, *325*, 427–437. [CrossRef]
32. Vatai, G.N.; Krstić, D.M.; Koris, A.K.; Gáspár, I.L.; Tekic, M.N. Ultrafiltration of oil-in-water emulsion: Comparison of ceramic and polymeric membranes. *Desalination Water Treat.* **2009**, *3*, 162–168. [CrossRef]